Acta Mech 229, 3901–3913 (2018)
https://doi.org/10.1007/s00707-018-2196-1

ORIGINAL PAPER

M. Yu · X. H. Peng · P. H. Wen

Effect of cooperative grain boundary sliding and migration on dislocation emission from interface collinear crack tip in nanocrystalline bi-materials

Received: 18 December 2017 / Revised: 13 April 2018 / Published online: 25 June 2018

Abstract The theoretical model of an edge dislocation near interface collinear crack tips in nanocrystalline bi-materials with cooperative grain boundary sliding and migration is formulated. As a typical example, we focus on analyzing the effect of two disclination dipoles produced by cooperative grain boundary sliding and migration on an edge dislocation emitting from a finite interfacial crack tip in nanocrystalline bi-materials. The dislocation force and the critical stress intensity factors for an edge dislocation emitting from an interface collinear crack tip under remote plane loadings are derived by using the complex potential method. And the influences of grain size, disclination strength, migration distance, sliding distance and interface crack length on the critical stress intensity factors are discussed in detail. It can be found that the effect of cooperative grain boundary sliding and migration deformation on the dislocation emission from interface collinear crack tip lies in the crack length, the dislocation emission angle, and the strength of the cooperative deformation itself.

1 Introduction

Nanocrystalline (NC) materials are the most spectacular materials in the field of materials science, and regarded as the most promising materials in the twenty-first century due to their excellent mechanical properties, such as superior strength, hardness, superplasticity, and wear resistance. Now, NC materials play an irreplaceable role in severe environments such as under ultra-high temperature and strong corrosion [1–12]. But at the same time, low tensile ductility and fracture toughness considerably limit their practical application in many cases [13–15]. Therefore, many scholars devote themselves to solving the difficult problem of how to combine good ductility with the superior strength of NC materials. A series of studies and reports show that some NC materials can have high strength and high fracture toughness at the same time due to their special deformation mechanism, such as rotational deformation, grain boundary sliding, migration of grain boundaries, triple junction diffusional creep, Coble creep, and nanoscale deformation twinning [10–26].

In recent years, researchers have paid close attention to the cooperative grain boundary sliding and migration, a deformed operation mode in NC solids [24–30]. The process includes the cooperative grain boundary sliding and stress-driven grain boundary migration near the tips of growing cracks. As is well known, grain

M. Yu
Hunan Provincial Key Laboratory of Engineering Rheology, Central South University of Forestry and Technology, Changsha 410004, China

X. H. Peng (✉)
Swan College of Central South University of Forestry and Technology, Changsha 410004, China
E-mail: pxh10000@163.com
Tel.: +86-731-85623347

P. H. Wen
School of Engineering and Material Sciences, Queen Mary, University of London, London E1 4NS, UK

boundary sliding is an important deformation mechanism as well as one of the specific deformation modes showing superplasticity in NC materials. But non-accommodated grain boundary sliding will produce dislocations and disclination dipoles at triple junctions of grain boundaries and form cracks, which lead to the embrittlement of NC materials. Conversely, if grain boundary sliding is effectively accommodated through diffusion, rotational deformation or lattice dislocations emitting from triple junctions, the NC material will show enhanced ductility or superplasticity. Grain boundary migration, another toughening micromechanism and specific deformation mode in NC materials, is suggested to be an effective way to accommodate grain boundary sliding. Therefore, the cooperative grain boundary sliding and migration is more able to explain the toughening mechanisms compared to pure grain boundary sliding and pure grain boundary migration in NC materials. In the suggested cooperative process, defects created by grain boundary sliding are partly accommodated by defects created by grain boundary migration. Ovid'ko and Sheinerman [27] studied the effect of cooperative grain boundary sliding and migration on crack growth in nanocrystalline solids, and found that the cooperative deformation increases the critical stress intensity factor for crack growth in nanocrystalline materials by a factor of three or more and thus considerably enhances the fracture toughness of such materials. Babicheva and Zhou [28] considered the effect of grain boundary segregation on the deformation mechanisms and mechanical properties of nanocrystalline binary aluminum alloys. The previous experimental and theoretical results show that the mechanism considerably enhances the fracture toughness of NC materials [24–34].

Most of the works, including lots of experimental and theoretical analyses, are focussed on the contribution of these special deformations to the toughening of NC materials, and little attention is paid to the influence of these special deformation mechanisms on the dislocation emission at the crack tips [24–34]. However, various defects are inevitable in NC solids, such as nano-holes, cracks, inclusions, and so on. In particular, as long as the stress intensity factor of crack tips is large enough, lattice dislocations will emit from crack tips, leading to plastic shear and hindering crack growth, thus improving the toughness of NC solids. For this reason, the influences of these special deformation mechanisms on lattice dislocations emitting from various crack tips are worth studying. So it is of great significance to study the effects of the cooperative grain boundary sliding and migration on the emission of lattice dislocations from various crack tips.

The key technology of designing a multiphase material with special performance is to solve the interface problem in heterogeneous materials. Due to differences in the nature of the two materials, the interface will inevitably have some defects, and these defects will become the source of cracks and thus lead to the destruction and fracture of NC bi-materials. In order to prevent the occurrence of fracture failure of nano-composite materials and prolong the service life, it is particularly important to study interface cracks propagation problems [28–35]. In this work, the effect of cooperative grain boundary sliding and migration on the lattice dislocation emission from interface collinear crack tips in NC bi-materials is quantitatively investigated. The dislocation force and the critical stress intensity factors corresponding to dislocation emitting from interface crack tips under remote plane loadings are deduced by using theory of Elasticity. And influences of grain size, interface crack length and characteristics of the cooperative grain boundary sliding and migration on the critical stress intensity factors are discussed in detail.

2 Problem description and model building

Consider a deformed infinite NC bi-material solid containing a large number of nanoscale grains separated by grain boundaries under remote model I and mode II loadings. The NC solid is divided into two planes by a planar interface with a series of interfacial collinear cracks along the plane $y = 0$. The cracks are deemed to be flat and plane, and the same width along the coordinate axis z perpendicular to the xy plane. The solid in the upper half (s^+, $y > 0$) is denoted by the subscript 1 and that in the lower half (s^-, $y < 0$) by the subscript 2. Both s^+ and s^- are isotropic, so the problem is treated as two-dimensional in the present work. Let L_j ($j = 0, 1, 2, \ldots$) denote the interface collinear cracks with the tips at points a_j, b_j lying along the interface ($y = 0$), and L the union of the crack segments L_j while L' represent the rest of the interface that fully bonded. In this case, the boundary condition along the interface can be written as [35,36]

$$u_1^+(t) + iv_1^+(t) = u_2^-(t) + iv_2^-(t) \qquad t \in L, \tag{1}$$

$$\sigma_{yy1}^+(t) - i\sigma_{xy1}^+(t) = \sigma_{yy2}^-(t) - i\sigma_{xy2}^-(t) \qquad t \in L', \tag{2}$$

$$\sigma_{yy1}^+(t) - i\sigma_{xy1}^+(t) = 0 \qquad t \in L, \tag{3}$$

$$\sigma_{yy2}^{-}(t) - i\sigma_{xy2}^{-}(t) = 0 \qquad t \in L, \tag{4}$$

where u, v are the displacement in the x-, y-direction and σ_{xxi}, σ_{yyi} the stress component, respectively, where $i = 1, 2$ under the condition of plane strain.

For plane strain problems, the stress field σ_{xx}, σ_{yy}, σ_{xy} and displacement field u, v can be generally expressed by two complex analytic potentials $\Phi(z)$ and $\Psi(z)$ as follows [37]:

$$\sigma_{yy} + i\sigma_{xy} = 2\left[\Phi(z) + \overline{\Phi(z)}\right], \tag{5}$$

$$\sigma_{yy} - \mathrm{i}\sigma_{xy} = \Phi(z) + \overline{\Phi(z)} + z\overline{\Phi'(z)} + \overline{\Psi(z)}, \tag{6}$$

$$2\mu\left(u'_{+}v'\right) = (3 - 4\upsilon)\Phi(z) - \overline{\Phi(z)} - z\overline{\Phi'(z)} - \Psi(z), \tag{7}$$

where $u' = \partial u/\partial x$, $v' = \partial v/\partial x$, $\Phi'(z) = \mathrm{d}\Phi(z)/\mathrm{d}z$, $i = \sqrt{-1}$, $z = x + iy$, and the overbar denotes the complex conjugate.

Both grain boundary sliding and migration can be induced near the crack tip under external load and internal high stress concentration. The cooperative deformation leads to two disclination dipoles *CD* and *BE*. At the same time, high stress concentration at the crack tip leads to the launch of a lattice dislocation, simplistically, assuming a lattice dislocation with only edge features.

Figure 1 schematically depicts the geometry of the cooperative grain boundary sliding and migration deformation. The vertical and horizontal distance between the triple junction A and a crack tip is p and p', respectively. The initial length of all grain boundaries is assumed as d. The vertical grain boundary A_2B_2 is perpendicular to the direction of the crack growth and at an angle φ with the grain boundaries A_2B_2 and B_2B_3. Both the strength of the two disclination dipoles *CD* and B_2E are set to ω, and the dipole arm length are $|x_1 - y_1|$ and y_1, respectively, where x_1 indicates the distance of the grain boundary sliding and y_1 the distance of the migration.

Two coordinate systems are introduced, one is a Cartesian coordinate system (x, y) with the origin point at o, the other is a Polar coordinate system (r, θ) with the origin point at o_1. Then, the four disclination positions D, C, B_2, E in the Cartesian coordinate system can be written as $z_1\left(= b_0 + p' + r_1e^{i\theta_1}\right)$, $z_2\left(= b_0 + p' + r_2e^{i\theta_2}\right)$, $z_3\left(= b_0 + p' + r_3e^{i\theta_3}\right)$, $z_4\left(= b_0 + p' + r_4e^{i\theta_4}\right)$, where $r_1 = \sqrt{y_1^2 + p^2 - 2y_1 p\cos\varphi}$, $r_2 = \sqrt{x_1^2 + p^2 - 2x_1 p\cos\varphi}$, $r_3 = p + d$, $r_4 = \sqrt{y_1^2 + (p+d)^2 - 2y_1(p+d)\cos\varphi}$, $\theta_1 = -\arccos(y_1\sin\varphi/r_1)$, $\theta_2 = -\arccos(x_1\sin\varphi/r_2)$, $\theta_3 = -\pi/2$, $\theta_4 = -\arccos(y_1\sin\varphi/r_4)$ [34–36].

3 Emission of an edge dislocation at collinear interface crack tip

Here, we only consider dislocations of edge character with their Burgers vectors lying along a slip plane making an angle θ_0 with the axis $y = 0$. Supposing the first edge dislocation emitting at a collinear interface crack tip locate in the lower half plane of $z_0 = b_0 + r_0\mathrm{e}^{\mathrm{i}\theta_0}$, and referring to the work of Zhang [37], the complex potentials $\Phi_2^e(z)$, $\Psi_2^e(z)$ can be written as

$$\Phi_2^e(z) = \Phi_{20}^e(z) + \Phi_{2*}^e(z) \qquad z \in s^-, \tag{8}$$

$$\Psi_2^e(z) = \Psi_{20}^e(z) + \Psi_{2*}^e(z) \qquad z \in s^-, \tag{9}$$

where $\Phi_{20}^e(z) = \frac{\gamma_2}{z - z_0}$, $\Psi_{10}^e(z) = \frac{\bar{\gamma}_2}{z - z_0} + \frac{\gamma_2\bar{z}_0}{(z - z_0)^2}$, $\gamma_2 = \frac{\mu_2}{4\pi(1-\upsilon_2)}\left(b_y - \mathrm{i}b_x\right)$.

Referring to [34], when only one finite collinear crack lies in the interface, with the tips at points a_0 and b_0, then the complex potential function $\Phi_2^e(z)$and $\Psi_2^e(z)$ can be denoted as

$$\begin{aligned}\Phi_2^e(z) = {} & h_2\left[\frac{\gamma_2}{z - z_0} - \frac{\gamma_2}{z - \bar{z}_0} - \frac{\bar{\gamma}_2(z_0 - \bar{z}_0)}{(z - \bar{z}_0)^2}\right] + h_1\frac{X_0(z)}{X_0(z_0)}\frac{\gamma_2}{z - z_0} + h_1(1 - g)\gamma_2 X_0(z) \\ & + h_1\frac{X_0(z)}{X_0(\bar{z}_0)}\left[\frac{\gamma_2}{z - \bar{z}_0} - \frac{\bar{\gamma}_2(\bar{z}_0 - z_0)}{(z - \bar{z}_0)^2} - \frac{\bar{z}_0 - \frac{1}{2}(a_0 + b_0) + i\beta(a_0 - b_0)}{(\bar{z}_0 - a)(\bar{z}_0 - b)}\frac{\bar{\gamma}_2(\bar{z}_0 - z_0)}{(z - \bar{z}_0)}\right], \end{aligned} \tag{10}$$

$$\Phi_2^{e'}(z) = h_2\left[-\frac{\gamma_2}{(z - z_0)^2} + \frac{\gamma_2}{(z - \bar{z}_0)^2} + \frac{2\bar{\gamma}_2(z_0 - \bar{z}_0)}{(z - \bar{z}_0)^3}\right] + h_1\frac{X_0'(z)}{X_0(z_0)}\frac{\gamma_2}{z - z_0} - h_1\frac{X_0(z)}{X_0(z_0)}\frac{\gamma_2}{(z - z_0)^2}$$

$$+h_1\frac{X_0'(z)}{X_0(\bar{z}_0)}\left[\frac{\gamma_2}{z-\bar{z}_0}-\frac{\bar{\gamma}_2(\bar{z}_0-z_0)}{(z-\bar{z}_0)^2}-\frac{\bar{z}_0-\frac{1}{2}(a_0+b_0)+i\beta(a_0-b_0)}{(\bar{z}_0-a)(\bar{z}_0-b)}\frac{\bar{\gamma}_2(\bar{z}_0-z_0)}{(z-\bar{z}_0)}\right]$$
$$+h_1(1-g)\gamma_2X_0'(z)$$
$$+h_1\frac{X_0(z)}{X_0(\bar{z}_0)}\left[-\frac{\gamma_2}{(z-z_0)^2}+\frac{2\bar{\gamma}_2(\bar{z}_0-z_0)}{(z-\bar{z}_0)^3}+\frac{\bar{z}_0-\frac{1}{2}(a_0+b_0)+i\beta(a_0-b_0)}{(\bar{z}_0-a)(\bar{z}_0-b)}\frac{\bar{\gamma}_2(\bar{z}_0-z_0)}{(z-\bar{z}_0)^2}\right], \tag{11}$$

$$\begin{aligned}\Psi_2^e(z)&=-\Phi_2^e(z)-z\bar{\Phi}_2^{e'}(z)-\bar{\Phi}_2^e(z)\\&=-\Phi_2^e(z)-z\bar{\Phi}_2^{e'}(z)+h_2\left[\frac{\bar{\gamma}_2}{z-\bar{z}_0}-\frac{\bar{\gamma}_2}{z-z_0}-\frac{\gamma_2(\bar{z}_0-z_0)}{(z-z_0)^2}\right]\\&\quad+h_1\frac{\overline{X_0}(z)}{\overline{X_0}(z_0)}\frac{\bar{\gamma}_2}{z-\bar{z}_0}+h_1(1-g)\gamma_2\overline{X_0}(z)\\&\quad+h_1\frac{\overline{X_0}(z)}{\overline{X_0}(\bar{z}_0)}\left[\frac{\bar{\gamma}_2}{z-z_0}-\frac{\gamma_2(z_0-\bar{z}_0)}{(z-z_0)^2}-\frac{z_0-\frac{1}{2}(a_0+b_0)-i\beta(a_0-b_0)}{(z_0-a)(z_0-b)}\frac{\gamma_2(z_0-\bar{z}_0)}{(z-z_0)}\right],\end{aligned} \tag{12}$$

where $h_2=\frac{4\mu_2(1-\nu_1)}{\mu_2(1-\nu_1)+\mu_1(1-\nu_2)}$, $h_1=\frac{4\mu_1(1-\nu_2)}{\mu_1(1-\nu_2)+\mu_2(1-\nu_1)}$.

Using the Peach-Koehler formula [39,40], the image force can be expressed as

$$\begin{aligned}f_{\text{image}}&=f_x^e-\mathrm{i}f_y^e=\left[\widehat{\sigma}_{xy}b_x+\widehat{\sigma}_{yy}b_y\right]+\mathrm{i}\left[\widehat{\sigma}_{xx}b_x+\widehat{\sigma}_{xy}b_y\right]\\&=\frac{\mu b^2}{4\pi(1-\nu_2)}\left(\frac{\Phi_e^*(z_0)+\overline{\Phi_e^*(z_0)}}{\gamma_2}+\frac{\bar{z}_0\Phi_e^{*'}(z_0)+\Psi_e^*(z_0)}{\bar{\gamma}_2}\right),\end{aligned} \tag{13}$$

where $\widehat{\sigma}_{xx}$, $\widehat{\sigma}_{yy}$ and $\widehat{\sigma}_{xy}$ are the perturbation stress components, and $\Phi_e^*(z_0)=\lim\limits_{z\to z_0}\left[\Phi_2^e(z)-\Phi_{20}^e(z)\right]$, $\Phi_e^{*'}(z_0)=\lim\limits_{z\to z_0}\frac{\mathrm{d}[\Phi_2^e(z)-\Phi_{20}^e(z)]}{\mathrm{d}z}$, $\Psi_e^*(z_0)=\lim\limits_{z\to z_0}\left[\Psi_2^e(z)-\Psi_{e0}(z)\right]$. If the edge dislocation is in the upper half, the superscript 1 and 2 in Eqs. (8)–(13) are exchanged.

4 The effect of cooperative grain boundary sliding and migration on edge dislocation emission

In the derivation process, two disclination dipoles produced by cooperative grain boundary sliding and migration are assumed to be located in the lower half plane, so the complex potentials $\Phi_2^\omega(z)$ and $\Psi_2^\omega(z)$ are divided into two parts as

$$\Phi_2^\omega(z)=\Phi_{20}^\omega(z)+\Phi_{2*}^\omega(z)\qquad z\in s^-, \tag{14}$$
$$\Psi_2^\omega(z)=\Psi_{20}^\omega(z)+\Psi_{2*}^\omega(z)\qquad z\in s^-, \tag{15}$$

where $\Phi_{20}^\omega(z)$, $\Psi_{20}^\omega(z)$ indicate the presence of two disclination dipoles produced by cooperative sliding and migration in the lower half plane without cracks, and the holomorphic complex potentials $\Phi_{2*}^\omega(z)$, $\Psi_{2*}^\omega(z)$ denote the interaction of the two disclination dipoles with collinear interfacial cracks. Referring to references [35–40], we have

$$\Phi_{20}^\omega(z)=\frac{D_2\omega}{2}\sum_{k=1}^{4}s_k\ln(z-z_k)\quad z\in s^-, \tag{16}$$

$$\Psi_{20}^\omega(z)=-\frac{D_2\omega}{2}\sum_{k=1}^{4}s_k\frac{\bar{z}_k}{z-z_k}\quad z\in s^-, \tag{17}$$

where $D_2=\frac{\mu_2}{2\pi(1-\nu_2)}$, $s_k=1(k=1,4)$, $s_k=$ -1$(k=2,3)$, z_k $(k=1,\ 2,3,4)$ represent the locations of four wedge disclination, and μ and ν are the shear modulus and Poisson's ratio, respectively.

Consider a special case where the interface contains only a finite length crack and where, without loss of generality, the crack tips are set as a_0 and b_0; then the complex potential functions $\Phi_2^{\omega}(z)$ and $\Psi_2^{\omega}(z)$ are eventually obtained as [35]

$$\begin{aligned}\Phi_2^{\omega}(z) = {} & \frac{D_2\omega}{2}\cdot\frac{1-g+h}{1-g}\sum_{k=1}^{4}s_k\left[\ln\frac{z-z_k}{z-\bar{z}_k}-\frac{z-z_k}{z-\bar{z}_k}\right]\\ & -\frac{D_2\omega}{2}\cdot\frac{hX_0(z)}{1-g}\cdot\sum_{k=1}^{4}s_k\left\{\frac{\ln(z-z_k)}{X_0(z_k)}+g(z_k-\bar{z}_k)-\frac{1}{X_0(\bar{z}_k)}\left[\frac{z-z_k}{z-\bar{z}_k}+\ln(z-\bar{z}_k)\right]\right\},\end{aligned} \tag{18}$$

$$\begin{aligned}\Phi_2^{\omega'}(z) = {} & \frac{D_2\omega}{2}\cdot\frac{1-g+h}{1-g}\sum_{k=1}^{4}s_k\left[\frac{1}{z-z_k}-\frac{2}{z-\bar{z}_k}+\frac{z-z_k}{(z-\bar{z}_k)^2}\right]\\ & -\frac{D_2\omega}{2}\cdot\frac{hX_0'(z)}{1-g}\cdot\sum_{k=1}^{4}s_k\left\{\frac{\ln(z-z_k)}{X_0(z_k)}+g(z_k-\bar{z}_k)-\frac{1}{X_0(\bar{z}_k)}\left[\frac{z-z_k}{z-\bar{z}_k}+\ln(z-\bar{z}_k)\right]\right\}\\ & -\frac{D_2\omega}{2}\cdot\frac{hX_0(z)}{1-g}\sum_{k=1}^{4}s_k\left\{\frac{1}{X_0(z_k)(z-z_k)}-\frac{1}{X_0(\bar{z}_k)}\left[\frac{2}{z-\bar{z}_k}-\frac{z-z_k}{(z-\bar{z}_k)^2}\right]\right\},\end{aligned} \tag{19}$$

$$\begin{aligned}\Psi_2^{\omega}(z) = {} & -\Phi_2^{\omega}(z)-z\bar{\Phi}_2^{\omega'}(z)-\bar{\Phi}_2^{\omega}(z)\\ = {} & -\Phi_2^{\omega}(z)-z\bar{\Phi}_2^{\omega'}(z)-\frac{D_2\omega}{2}\cdot\frac{1-g+h}{1-g}\sum_{k=1}^{4}s_k\left[\ln\frac{z-\bar{z}_k}{z-z_k}-\frac{z-\bar{z}_k}{z-z_k}\right]\\ & +\frac{D_2\omega}{2}\cdot\frac{h\overline{X_0}(z)}{1-g}\sum_{k=1}^{4}s_k\left\{\frac{\ln(z-\bar{z}_k)}{\overline{X_0(z_k)}}+g(\bar{z}_k-z_k)-\frac{1}{\overline{X_0(\bar{z}_k)}}\left[\frac{z-\bar{z}_k}{z-z_k}+\ln(z-\bar{z}_k)\right]\right\},\end{aligned} \tag{20}$$

where $g=-\frac{\mu_1+\mu_2(3-4\nu_1)}{\mu_2+\mu_1(3-4\nu_2)}$, $h=-\frac{4\mu_1(1-\nu_2)}{\mu_2+\mu_1(3-4\nu_2)}$, $X_0(z)=(z-a_0)^{-0.5-i\beta}(z-b_0)^{-0.5+i\beta}$, $\beta=\frac{\ln|g|}{2\pi}$, $X_0'(z)=\frac{\mathrm{d}X_0(z)}{\mathrm{d}z}$.

So the force of the cooperative grain boundary sliding and migration on the edge dislocation can be written as [39]

$$\begin{aligned}f_{\text{wedge}} = {} & f_x^{\omega}-\mathrm{i}f_y^{\omega}=\left[\sigma_{xy}(z_0)b_x+\sigma_{yy}(z_0)b_y\right]+\mathrm{i}\left[\sigma_{xx}(z_0)b_x+\sigma_{xy}(z_0)b_y\right]\\ = {} & \frac{\mu_2 b^2}{4\pi(1-\nu_2)}\left(\frac{\Phi_2^{\omega}(z_0)+\overline{\Phi_2^{\omega}(z_0)}}{\gamma_2}+\frac{\bar{z}_0\Phi_2^{\omega'}(z_0)+\Psi_2^{\omega}(z_0)}{\bar{\gamma}_2}\right),\end{aligned} \tag{21}$$

where σ_{xx}, σ_{yy} and $\sigma_{xy}$are the stress-filed components produced by the cooperative grain boundary sliding and migration .

When the cooperative grain boundary sliding and migration emerges in the upper half, the two complex potentials are obtained by exchanging the subscripts 1 and 2 in Eqs. (14)–(21).

5 The external force acting on edge dislocation emission

In this part, we discuss the force of remote model I and mode II loadings on the edge dislocation:

$$f_{\Gamma}=b\sigma_{r\theta}, \tag{22}$$

where $\sigma_{r\theta}=\left(\sigma_y-\sigma_x\right)\sin\theta\cos\theta+\sigma_{xy}\left(\cos^2\theta-\sin^2\theta\right)$ is the in-plane shear stress under external load.

For linear elastic plane problems, Irwin (1957) has obtained the well-known stress field formula of a sharp crack tip only considering the expansion of the first item [35–42].

$$\begin{Bmatrix}\sigma_x\\ \sigma_y\\ \sigma_{xy}\end{Bmatrix}=\frac{K_{\mathrm{Iapp}}}{\sqrt{2\pi r}}\cos\frac{\theta}{2}\begin{Bmatrix}1-\sin\frac{\theta}{2}\sin\frac{3\theta}{2}\\ 1+\sin\frac{\theta}{2}\sin\frac{3\theta}{2}\\ \sin\frac{\theta}{2}\cos\frac{3\theta}{2}\end{Bmatrix}+\frac{K_{\mathrm{IIapp}}}{\sqrt{2\pi r}}\begin{Bmatrix}-\sin\frac{\theta}{2}\left(2+\cos\frac{\theta}{2}\cos\frac{3\theta}{2}\right)\\ \sin\frac{\theta}{2}\cos\frac{\theta}{2}\cos\frac{3\theta}{2}\\ \cos\frac{\theta}{2}\left(1-\sin\frac{\theta}{2}\sin\frac{3\theta}{2}\right)\end{Bmatrix}, \tag{23}$$

where K_{Iapp} and K_{IIapp} are the generalized mode I and mode II stress intensity factors produced by the remote loadings.

So Eq. (22) can be written as

$$f_\Gamma=b\sigma_{r\theta}=\frac{b}{\sqrt{2\pi r_0}}\left(l_1K_{\mathrm{Iapp}}+l_2K_{\mathrm{IIapp}}\right), \tag{24}$$

where $l_1=\frac{1}{2}\sin\theta\cos\frac{\theta}{2}$, $l_2=\cos\frac{3\theta}{2}+\sin^2\frac{\theta}{2}\cos\frac{\theta}{2}$.

6 The critical stress intensity factors for the edge dislocation emission

In this analysis, the force acting on the edge dislocation contains three parts: image force, the cooperative grain boundary sliding and migration and the external force, so it can be expressed as

$$f_{\mathrm{emit}}=f_x\cos\theta+f_y\sin\theta+f_\Gamma=\mathrm{Re}[f_{\mathrm{image}}+f_{\mathrm{wedge}}]\cos\theta-\mathrm{Im}\left[f_{\mathrm{image}}+f_{\mathrm{wedge}}\right]\sin\theta+f_\Gamma. \tag{25}$$

Substituting Eqs. (13), (21) and (24) into Eq. (25), the expression of the dislocation emission force can be obtained.

That the dislocation will emit from crack tips when the force acts on dislocation equal to zero and the dislocation distance to the crack surface must be equal to, or larger than, the dislocation core radius, is a well-known accepted emission criterion [41,42]. Let $f_{\mathrm{emit}}=0$, and then the critical stress intensity factor $K_{\mathrm{IC}}^{\mathrm{app}}$ and $K_{\mathrm{IIC}}^{\mathrm{app}}$ for the dislocation emission can be derived as follows:

$$K_{\mathrm{II}}^{\mathrm{app}}=0,\quad K_{\mathrm{IC}}^{\mathrm{app}}=\frac{\sqrt{2\pi r_0}}{bl_1}\left(\mathrm{Im}\left[f_{\mathrm{image}}+f_{\mathrm{wedge}}\right]\sin\theta-\mathrm{Re}\left[f_{\mathrm{image}}+f_{\mathrm{wedge}}\right]\cos\theta\right), \tag{26}$$

$$K_{\mathrm{I}}^{\mathrm{app}}=0,\quad K_{\mathrm{IIC}}^{\mathrm{app}}=\frac{\sqrt{2\pi r_0}}{bl_2}\left(\mathrm{Im}\left[f_{\mathrm{image}}+f_{\mathrm{wedge}}\right]\sin\theta-\mathrm{Re}\left[f_{\mathrm{image}}+f_{\mathrm{wedge}}\right]\cos\theta\right), \tag{27}$$

where $f_{\mathrm{image}}+f_{\mathrm{wedge}}=\frac{\mu_2b^2}{4\pi(1-\nu_2)}\left\{\frac{2\mathrm{Re}[\Phi_e^*(z_0)+\Phi_w(z_0)]}{\gamma_2}+\frac{\bar{z}_0\left[\Phi_e^{*'}(z_0)+\Phi_w{}'(z_0)\right]+\left[\Psi_e^*(z_0)+\Psi_w(z_0)\right]}{\bar{\gamma}_2}\right\}$.

From previous studies [28–36], we found that the dislocations will easily emit from crack tips in softer materials, so in this paper we mainly discuss the effect of cooperative grain boundary sliding and migration near the crack tip on the emission of lattice dislocations from the collinear interface crack tip in the same half plane. In the following analysis, the critical normalized stress intensity factors (SIFs) are normalized as $K_{\mathrm{IC}}^0=K_{\mathrm{IC}}^{\mathrm{app}}/\mu_2\sqrt{b}$ and $K_{\mathrm{IIC}}^0=K_{\mathrm{IIC}}^{\mathrm{app}}/\mu_2\sqrt{b}$, and the emitting dislocation is located at $z_0=r_0e^{i\theta_0}$. Let the Burgers vector $b=0.25\,\mathrm{nm}$, $r_0=b/2$, $p'=0$, and the crack length is l.

Supposing the upper half is softer than the lower half, the cooperative grain boundary sliding and migration occurs in the upper half and the edge dislocation is emitted from a collinear interface crack in the upper half. The materials in the upper half and the lower half are set as nanocrystalline material Ni and 3C-SiC, respectively, so $\mu_1=73\,\mathrm{GPa}$, $\nu_1=0.31$, $\mu_2=217\,\mathrm{GPa}$, $\nu_2=0.23$.

With different disclination strengths, the dependences of the normalized critical SIFs with the dislocation emission angle are presented in Fig. 2. As illustrated in Fig. 2, when the cooperative grain boundary sliding and migration does not exist ($\omega\neq0^\circ$), K_{IC}^0 decreases first and then increases with increasing dislocation emission angle. In this case, the most probable angle for dislocation emission is 72.5° corresponding to the minimum value of the normalized critical SIF, which is in good agreement with the result in Ref. [35]. K_{IIC}^0 increases from a finite positive value to infinity and switches to negative with increasing emitting angle, so the most probable angle for positive dislocation emission is 0°, while it is 125.5° for negative dislocation emission, which is in good agreement with the result in Ref. [35].

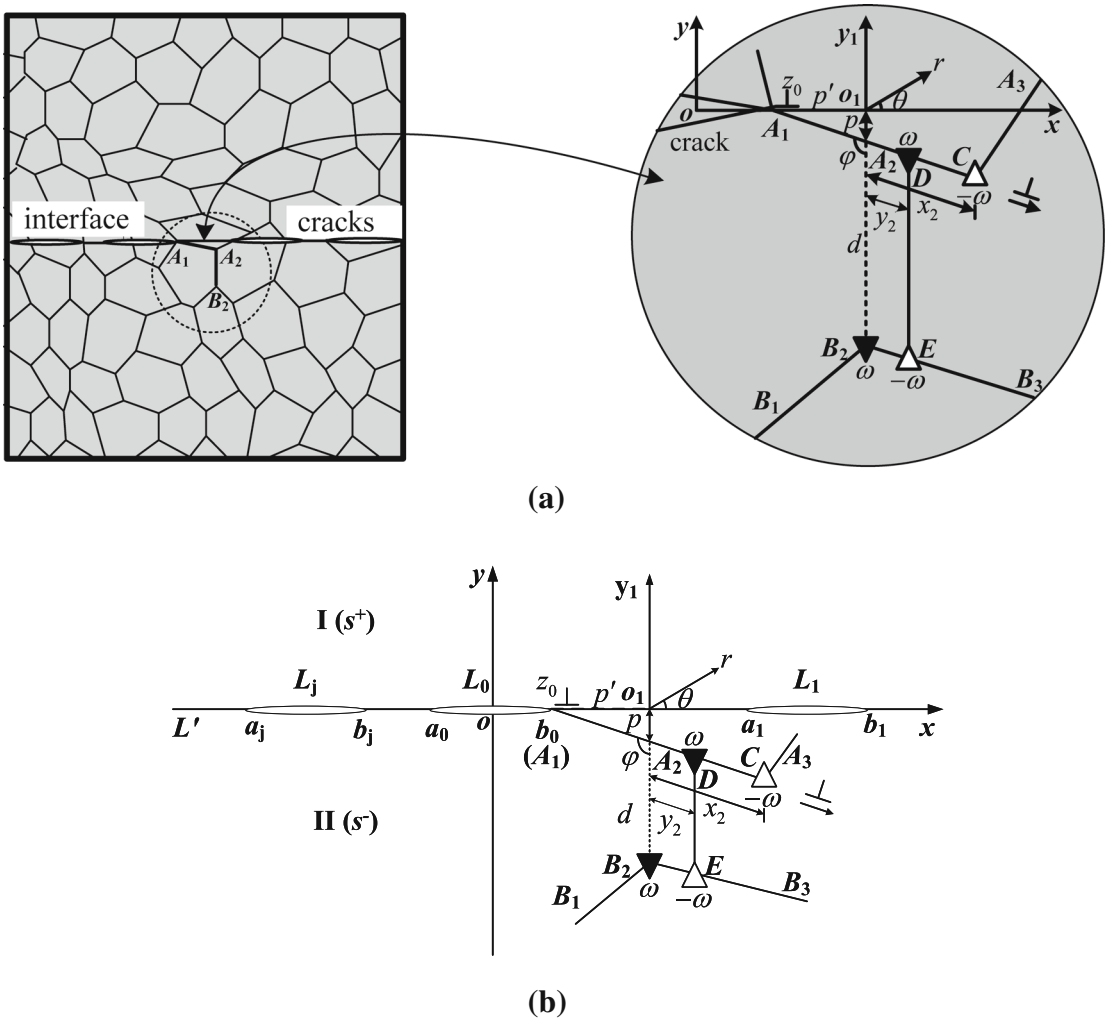

Fig. 1 The cooperative grain boundary sliding and migration deformation and the edge dislocation emitting from interfacial collinear crack tips in an NC solid. **a** Two-dimensional NC solid and the cooperative grain boundary sliding and migration deformation. **b** Computation model

When the cooperative grain boundary sliding and migration forms near the crack tip, K_{IC}^0 increases with increasing dislocation emission angle and transfer from negative dislocation emission into positive dislocation emission, so the most probable angles for dislocation emission are 26.5°, 34°, 38° when ω=30°, 45°, 60°, respectively, corresponding to K_{IC}^0 equal to zero. K_{IIC}^0 increases from a negative value to positive infinity and then turns to negative, the most probable angles for dislocation emission are the same as that of K_{IC}^0.

Figure 3 shows the dependences of the normalized critical K_{IC}^0 on the dislocation emission angle with different crack lengths. As is shown in Fig. 3, K_{IC}^0 first decreases and then increases with increasing the emission angle of dislocation when the collinear interface crack is relatively small, and increases from negative to positive when the crack is relatively large; obviously, there are the most probable angles for dislocation emission corresponding to the minimum value of K_{IC}^0 or $K_{IC}^0 = 0$. When the emission angle is relatively small, K_{IC}^0 changes from positive to negative with the increase in the crack length, so there is a critical crack length l_0 making $K_{IC}^0 = 0$. However, K_{IC}^0 decreases with increasing crack length.

With different disclination strengths, the variation of the normalized critical K_{IC}^0 with respect to the crack length is depicted in Fig. 4. It can be found that the influence of the collinear crack length on K_{IC}^0 is very small when the cooperative grain boundary sliding and migration does not exist or disappears ($\omega = 0°$), but when the cooperative grain boundary sliding and migration forms near the crack tip ($\omega \neq 0°$), K_{IC}^0 decreases with increasing crack length. It can be seen that dislocations are easier to emit from shorter cracks and the

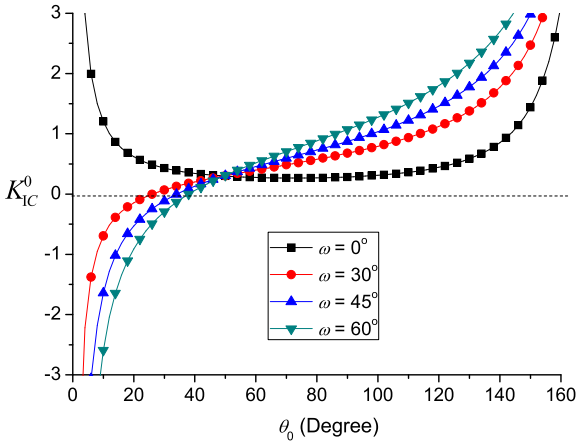

(a) K_{IC}^0

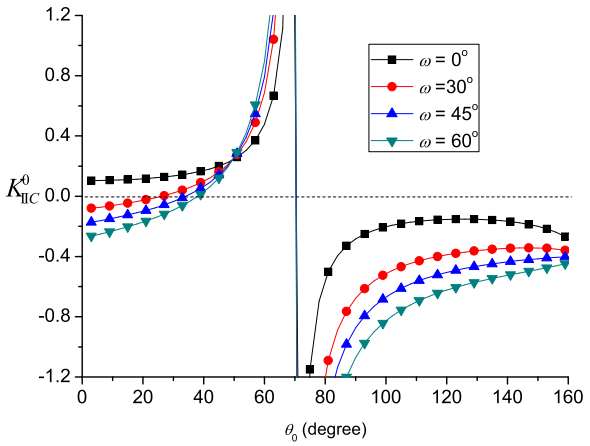

(b) K_{IIC}^0

Fig. 2 The variation of the normalized critical SIFs as the dislocation emission angle with different disclination strengths (l = 1000 nm, $x = 0.3d$ nm, $y = 0.1d$ nm, d = 12 nm, $p = d$, $\varphi = 120°$)

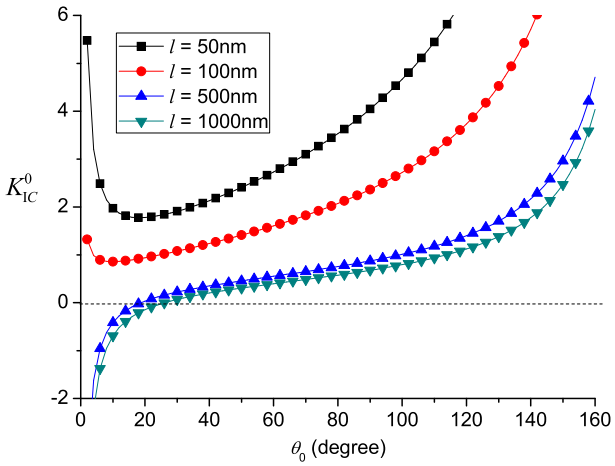

Fig. 3 The variation of the normalized critical K_{IC}^0 as the dislocation emission angle with different crack lengths ($x = 0.3d$ nm, $y = 0.1d$ nm, d = 12 nm, $p = d$, $\varphi = 120°$, $\omega = 30°$)

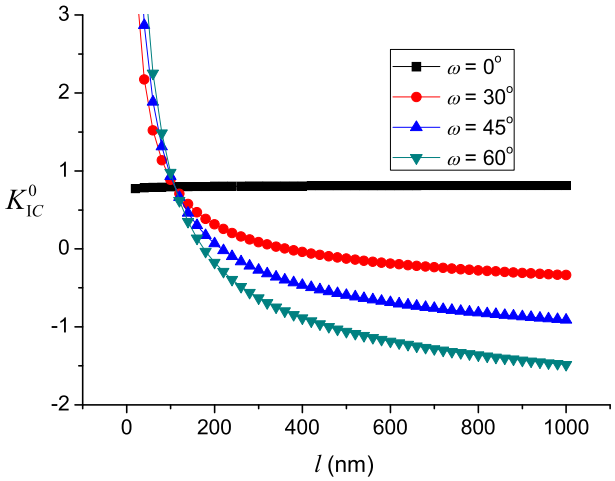

Fig. 4 The variation of the normalized critical K_{IC}^0 as the crack length with different disclination strengths ($x = 0.3d$ nm, $y = 0.1d$ nm, $d = 12$ nm, $p = d$, $\varphi = 120°$, $\theta_0 = 15°$)

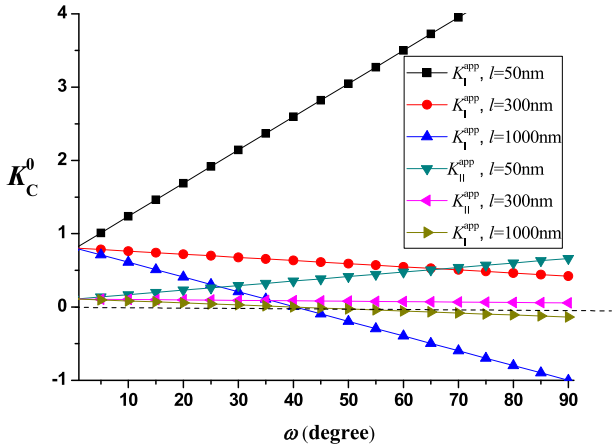

Fig. 5 The variation of the normalized critical SIFs as disclination strength ($x = 0.3d$ nm, $y = 0.1d$ nm, $d = 12$ nm, $p = d$, $\varphi = 120°$, $\theta_0 = 15°$)

longer cracks expand more easily. And when the interface collinear crack length is constant, K_{IC}^0 increases with increasing disclination strength. It is obvious that the cooperative grain boundary sliding and migration promote crack propagation in this case. And as the emission angle becomes small, K_{IC}^0 changes from positive to negative, so there exists a critical crack length l_0 making $K_{IC}^0 = 0$.

Figure 5 depicts the dependence of normalized critical SIFs on the disclination strength. It can be found that the normalized critical SIFs all increase with increasing disclination strength; here, the cooperative grain boundary sliding and migration hinders the dislocation emitting from a crack tip. On the contrary, when the interface collinear crack length is relatively long, the normalized critical SIFs decrease with increasing disclination strength, and the cooperative grain boundary sliding and migration promotes dislocation emission in this case. There exists critical disclination strength ω_0 making $K_C^0 = 0$, so dislocations will emit from crack tips without external loading as long as $\omega > \omega_0$. K_{IC}^0 is greater than K_{IIC}^0 under the same conditions, meaning that dislocations are easily to emit under model II loadings than under model I loadings. It is obvious that the effect of cooperative grain boundary sliding and migration deformation on the dislocation emission at the crack tip is either dependent on the crack length, the dislocation emission angle, or the strength of the cooperative deformation itself.

The dependence of the normalized critical K_{IC}^0 on the dislocation emission angle with different relative sliding distances are shown in Fig. 6. We can find that K_{IC}^0 changes from negative to positive with increasing emission angle, so there is a most probable angle for dislocation emission corresponding to K_{IC}^0 equal to

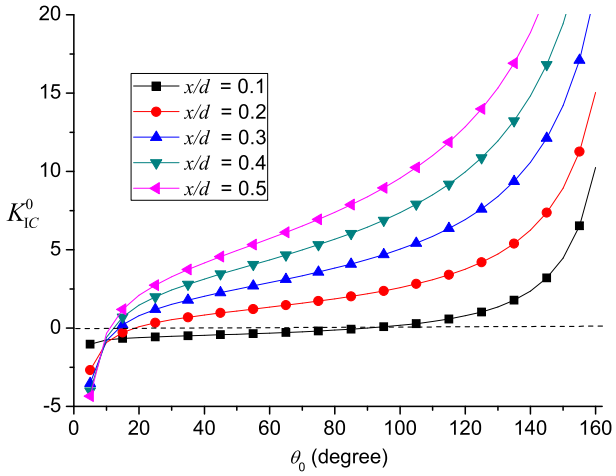

Fig. 6 The variation of the normalized critical K_{IC}^0 as the emission angle with different relative sliding distances ($l = 1000$ nm, $y/d = 0.1$, $d = 12$ nm, $p = d$, $\omega = 5°$, $\varphi = 120°$)

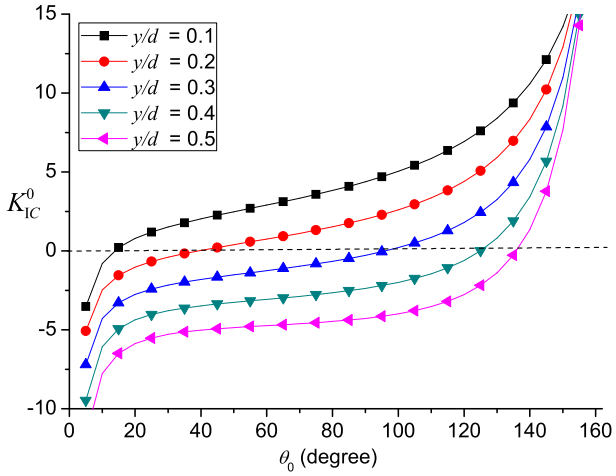

Fig. 7 The variation of the normalized critical K_{IC}^0 as the emission angle with different relative migration distances ($l = 1000$ nm, $x/d = 0.3$, $d = 12$ nm, $p = d$, $\omega = 5°$, $\varphi = 120°$)

zero, and the values of the most probable angles decrease as the sliding distance increases. Under the same conditions, increasing sliding distance can increase the value of K_{IC}^0, indicating that increasing sliding distance will hinder dislocation emission.

Figure 7 depicts the dependence of the normalized critical K_{IC}^0 on the emission angle with different relative migration distances. It can be found that K_{IC}^0 has the same variation law with increasing emission angle as it has in Fig. 6, and the most probable angle increases with increasing migration distance.

The dependence of the normalized critical K_{IC}^0 on the relative migration distance when the relative sliding distances is different is depicted in Fig. 8. It can be seen that K_{IC}^0 increases with increasing relative migration distance, and it increases with increasing the relative sliding distance if the migration distance is certain. So it is clear that the crystal boundary sliding hinders the dislocation emission, while crystal boundary migration promotes dislocation emission in this case.

Figure 9 depicts the variations of the normalized critical K_{IC}^0 with the grain size when grain boundary angles are different. It can be found that the normalized critical K_{IC}^0 decreases with increasing grain size. There is a critical grain size d_c making K_{IC}^0 equal to zero. As long as the grain size is larger than the critical grain size, the dislocation will emit from the crack tip without external loadings. And the normalized critical K_{IC}^0 decreases with increasing grain boundary angle φ.

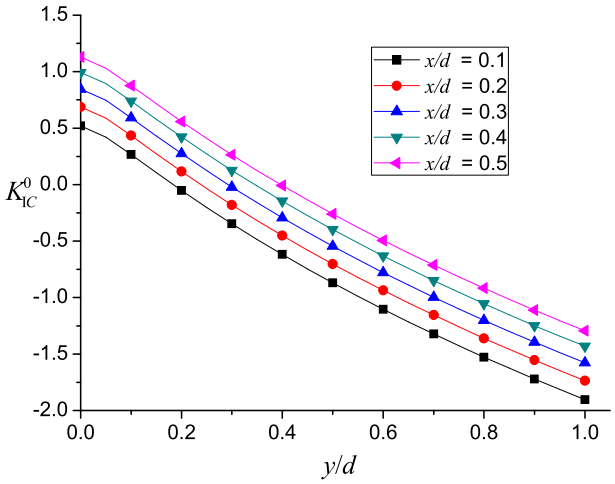

Fig. 8 The variation of the normalized critical K_{IC}^0 as the relative migration distance with different relative sliding distances ($l = 2000$ nm, $\theta_0 = 60°$, $d = 12$ nm, $p = d$, $\omega = 5°$, $\varphi = 120°$)

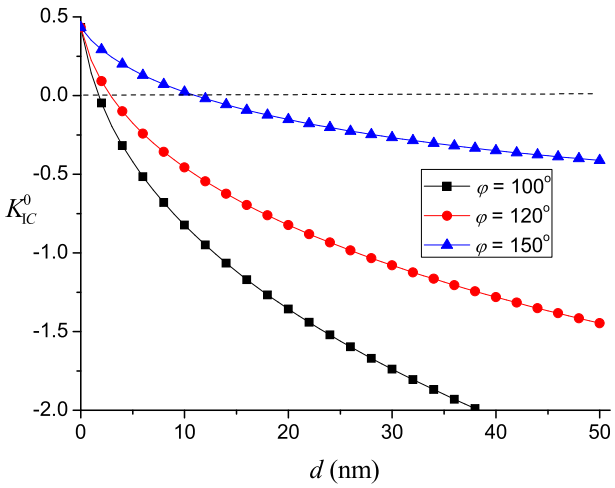

Fig. 9 The variation of the normalized critical K_{IC}^0 as the grain size with different grain boundary angles ($l = 1000$ nm, $\theta_0 = 60°$, $x = 0.3d$ nm, $y = 0.1d$ nm, $d = 12$ nm, $\omega = 30°$)

7 Conclusions

The interference law of cooperative grain boundary sliding and migration with interface collinear crack has been investigated in this paper, and its effect on the edge dislocation emitting from an interface crack tip is also studied in deformed nanocrystalline bi-materials. The analytic solutions of the model are deduced by the complex potential method of elasticity, and through numerical analysis, the influences of disclination strength, grain size, migration distance, sliding distance and interface crack length on the critical stress intensity factors corresponding to dislocation emission are discussed in detail.

1. There is the most probable angle for dislocation emission corresponding to the minimum value of critical stress intensity factor, and the most probable angle increases with increasing disclination strength when cooperative grain boundary sliding and migration deformation occurs near the collinear crack tip. When the emission angle is relatively small, there is a critical crack length that a dislocation can emit from the crack tip without external loadings.
2. K_{IC}^0 decreases with increasing crack length when the emission angle is relatively large. And when the cooperative grain boundary sliding and migration forms near the crack tip, K_{IC}^0 decreases with increasing crack length. It can be seen that if the interface collinear crack is short, cracks are more likely to emit dislocations, and if the interfaces collinear crack is longer, the cracks are easier to expand.

3. There exists a critical disclination strength making the generalized mode I stress intensity factor equal to zero, so dislocations will emit from crack tips without external loading as long as $\omega > \omega_0$. And dislocations are easier to emit under model II loadings than under model I loadings.
4. There is a critical grain size making the generalized mode I stress intensity factor equal to zero. As long as the grain size is larger than the critical grain size, the dislocation will emit from the crack tip without external loadings. And the normalized critical decreases with increasing grain boundary angle φ.
5. The grain boundary sliding of cooperative grain boundary sliding and migration prevents dislocation emission, while grain boundary migration promotes dislocation emission.

It can be seen that whether cooperative grain boundary sliding and migration deformation promotes or hinders dislocation emission at the interface collinear crack tip depends on the crack length, dislocation emission angle, and the strength of the synergistic deformation itself.

Acknowledgements The authors would like to deeply appreciate the support from the National Natural Science Foundation of China (Grant No. 11602308). The work was also supported by the Introducing High-level Talent Research Fund of Central South University of Forestry and Technology (104-0096).

References

1. Zhao, H.B., Feng, H., Liu, F., Liu, Y.W., Wen, P.H.: Effect of nanoscale twin and dislocation pileup at twin boundary on crack blunting in nanocrystalline materials. Acta Mech. **228**(10), 3483–3495 (2017)
2. He, T., Xiao, W., Zhang, Y., Zhu, H.: Effect of special rotational deformation on the dislocation emission from a branched crack tip in deformed nanocrystalline materials. Acta Mech. **228**(3), 823–836 (2017)
3. Zhao, J., Liu, J., Kang, G., An, L., Zhang, X.: The competitive nucleation of misfit dislocation dipole and misfit extended dislocation dipole in nanocomposites. Acta Mech. **228**(7), 2541–2554 (2017)
4. Zhao, Y.X., Fang, Q.H., Liu, Y.W.: Effect of nanograin boundary sliding on nanovoid growth by dislocation shear loop emission in nanocrystalline materials. Eur. J. Mech. A Solids **49**, 419–429 (2015)
5. Liu, Y.G., Ju, R.Y.: A theoretical model for studying the mechanical properties of bimodal nanocrystalline materials. J. Mater. Res. **30**(11), 1836–1843 (2015)
6. Wang, P., Yang, X.H., Tian, X.B.: Fracture behavior of precracked nanocrystalline materials with grain size gradients. J. Mater. Res. **30**(5), 709–716 (2015)
7. Nejadseyfi, O., Shamsborhan, M., Azimi, A., Shokuhfar, A.: The roles of crystallographic orientation, high-angle grain boundary, and indenter diameter during nano-indentation. Acta Mech. **226**(11), 3823 (2015)
8. Zhou, Q., Xie, J.Y., Wang, F., Huang, P., Xu, K.W., Lu, T.J.: The mechanical behavior of nanoscale metallic multilayers: A survey. Acta. Mech. Sin. **31**(3), 319–337 (2015)
9. Ovid'ko, I.A., Skiba, N.V.: Generation of nanoscale deformation twins at locally distorted grain boundaries in nanomaterials. Int. J. Plast. **62**, 50–71 (2014)
10. Zhou, K., Wu, M.S., Nazarov, A.A.: Relaxation of a disclinated tricrystalline nanowire. Acta Mater. **56**, 5828–5836 (2008)
11. Laursen, A.B., Patraju, K.R., Whitaker, M.J., et al.: Nanocrystalline Ni_5P_4: a hydrogen evolution electrocatalyst of exceptional efficiency in both alkaline and acidic media. Energy Environ. Sci. **8**(3), 1027–1034 (2015)
12. Zhou, K., Wu, M.S.: Elastic fields due to an edge dislocation in an isotropic film-substrate by the image method. Acta Mech. **211**(3–4), 271–292 (2010)
13. Kalidindi, A.R., Chookajorn, T., Schuh, C.A.: Nanocrystalline materials at equilibrium: a thermodynamic review. JOM **67**(12), 2834–2843 (2015)
14. Fang, Q.H., Feng, H., Liu, Y.W., Lin, S., Zhang, N.: Special rotational deformation effect on the emission of dislocations from a crack tip in deformed nanocrystalline solids. Int. J. Solids Struct. **49**, 1406–1412 (2012)
15. Zhou, K.: Elastic field and effective moduli of periodic composites with arbitrary inhomogeneity distribution. Acta Mech. **223**(2), 293–308 (2012)
16. Ovid'ko, I.A., Sheinerman, A.G., Valiev, R.Z.: Dislocation emission from deformation-distorted grain boundaries in ultrafine-grained materials. Scr. Mater. **76**, 45–48 (2014)
17. Ovid'ko, I.A., Skiba, N.V.: Nanotwins induced by grain boundary deformation processes in nanomaterials. Scr. Mater. **71**, 33–36 (2014)
18. Bobylev, S.V., Ovid'ko, I.A.: Stress-driven migration of deformation-distorted grain boundaries in nanomaterials. Acta Mater. **88**, 260–270 (2015)
19. Ovid'ko, I.A., Sheinerman, A.G.: Effects of incoherent nanoinclusions on stress-driven migration of low-angle grain boundaries in nanocomposites. J. Mater. Sci. **50**(12), 4430–4439 (2015)
20. Wang, L., Teng, J., Liu, P., Hirata, A., Ma, E., Zhang, Z., Han, X.: Grain rotation mediated by grain boundary dislocations in nanocrystalline platinum. Nat. Commun. **5**, 4402 (2014)
21. Zhao, Y.X., Zeng, X., Chen, C.P.: Elastic behavior of disclination dipole near nanotube with surface/interface effect. Chin. Phys. B **23**(3), 030202 (2014)
22. Yu, M., Fang, Q.H., Feng, H., Liu, Y.W.: Effect of special rotational deformation on dislocation emission from a semi-elliptical blunt crack tip in nanocrystalline solids. J. Mater. Res. **28**(6), 798–805 (2013)
23. Zhao, Y.X., Fang, Q.H., Liu, Y.W.: A wedge disclination dipole interacting with a coated cylindrical inhomogeneity. Acta Mech. Solida Sin. **28**(1), 62–73 (2015)

24. Feng, H., Lam, Y.C., Zhou, K., Kumar, S.B., Wu, W.J.: Elastic–plastic behavior analysis of an arbitrarily oriented crack near an elliptical inhomogeneity with generalized Irwin correction. Eur. J. Mech. A Solids **67**, 177–186 (2018)
25. Bobylev, S.V., Morozov, N.F., Ovid'ko, I.A.: Cooperative grain boundary sliding and migration process in nanocrystalline solids. Phys. Rev. Lett. **105**, 055504 (2010)
26. Ovid'ko, I.A., Sheinerman, A.G.: Free surface effects on stress-driven grain boundary sliding and migration processes in nanocrystalline materials. Acta Mater. **121**, 117–125 (2016)
27. Ovid'ko, I.A., Sheinerman, A.G., Aifantis, E.C.: Effect of cooperative grain boundary sliding and migration on crack growth in nanocrystalline solids. Acta Mater. **59**, 5023–5031 (2011)
28. Babicheva, R.I., Dmitriev, S.V., Bai, L.C., Zhang, Y., Kok, S.W., Kang, G.Z., Zhou, K.: Effect of grain boundary segregation on the deformation mechanisms and mechanical properties of nanocrystalline binary aluminum alloys. Comput. Mater. Sci. **117**, 445–454 (2016)
29. Feng, H., Fang, Q.H., Zhang, L.C., Liu, Y.W.: Effect of cooperative grain boundary sliding and migration on emission of dislocations from a crack tip in nanocrystalline materials. Mech. Mater. **61**, 39–48 (2013)
30. Feng, H., Fang, Q.H., Zhang, L.C., Liu, Y.W.: Special rotational deformation and grain size effect on fracture toughness of nanocrystalline materials. Int. J. Plast. **42**, 50–64 (2013)
31. Fang, Q.H., Zhang, L.C., Liu, Y.W.: Influence of grain boundary sliding and grain size on dislocation emission from a crack tip. Int. J. Damage Mech. **23**(2), 192–202 (2014)
32. Feng, H., Fang, Q.H., Liu, Y.W., Chen, C.P.: Nanoscale rotational deformation effect on dislocation emission from an elliptically blunted crack tip in nanocrystalline materials. Int. J. Solids Struct. **51**, 352–358 (2014)
33. Zhao, Y.X., Fang, Q.H., Liu, Y.W.: Effect of cooperative nanograin boundary sliding and migration on dislocation emission from a blunt nanocrack tip in nanocrystalline materials. Philos. Mag. **94**(7), 700–730 (2014)
34. Yu, M., Fang, Q.H., Feng, H., Liu, Y.W.: Effect of cooperative grain boundary sliding and migration on dislocation emitting from a semi-elliptical blunt crack tip in nanocrystalline solids. Acta Mech. **225**(7), 2005–2019 (2014)
35. Fang, Q.H., Liu, Y.W., Jiang, C.P., Li, B.: Interaction of a wedge disclination dipole with interfacial cracks. Eng. Fract. Mech. **73**, 1235–1248 (2006)
36. Yu, M., Fang, Q.H., Feng, H., et al.: Effect of special rotational deformation on dislocation emission from interface collinear crack tip in nanocrystalline bi-materials. Acta Mech. **227**(7), 2011–2024 (2016)
37. Muskhelishvili, N.L.: Soma Basic Problems of Mathematical Theory of Elasticity. Noordhoff, Leyden (1975)
38. Zhang, T.Y., Li, J.C.M.: Interaction of an edge dislocation with an interfacial crack. J. Appl. Phys. **72**, 2215–2226 (1992)
39. Hirth, J.P., Lothe, J.: Theory of Dislocations, vol. 2. Wiley, New York (1964)
40. Creager, M., Paris, P.C.: Elastic field equations for blunt cracks with reference to stress corrosion cracking. Int. J. Fract. **3**, 247–252 (1967)
41. Rice, J.R., Thomson, R.: Ductile versus brittle behavior of crystals. Philos. Mag. **29**, 73–80 (1974)
42. Fang, Q.H., Zhang, L.C.: Prediction of the threshold load of dislocation emission in silicon during nanoscratching. Acta Mater. **61**, 5469–5476 (2013)